Optical add-drop filters based on photonic crystal ring resonators

Zexuan Qiang, Weidong Zhou

Department of Electrical Engineering, NanoFAB Center, University of Texas at Arlington, Arlington, TX 76019-0072
wzhou@uta.edu

Richard A. Soref

Sensors Directorate, Air Force Research Laboratory, AFRL/SNHC, Hanscom Air Force Base, MA 01731-2909
Richard.Soref@hanscom.af.mil

Abstract: We present here an optical add-drop filter (ADF) design based on ultra-compact photonic crystal ring resonators (PCRRs). The normalized transmission spectra for single-ring and dual-ring configurations have been investigated by using the two-dimensional finite-difference time-domain (FDTD) technique in a square lattice dielectric-rod photonic-crystal structure. With the introduction of four scatterers at the corners of quasi-square-ring PCRR, high wavelength selectivity and close to 100% drop efficiency can be obtained. Both backward- and forward-dropping were achieved by controlling the coupling efficiency between two PCRR rings for resonant modes with different symmetry. The resonant-mode quality factor Q and the wavelength tunability were also analyzed, opening opportunities for PCRRs as ultra-compact filters, optical add-drop multiplexers, electrooptical N x N switches and electrooptical modulators.

OCIS codes: (230.0230) Optical devices; (250.5300) Photonic integrated circuits; (130.3130) Integrated optics materials; (230.7390) Waveguides; (060.1810) Couplers, switches, and multiplexers; (999.9999) Photonic crystals

References and links

1. R. A. Soref, "Silicon-based optoelectronics," Proc. IEEE **81,** 1687-1706 (1993).
2. B. E. Little, S. T. Chu, H. A. Haus, J. Foresi, and J. P. Laine, "Microring resonator channel dropping filters," J. Lightwave Technol. **15,** 998-1005 (1997).
3. S. Fan, P. R. Villeneuve, and J. D. Joannopoulos, "Channel drop filters in photonic crystals," Opt. Express **3,** 4-11 (1998).
4. M. Lipson, "Guiding, Modulating and Emitting Light on Silicon - Challenges and Opportunities (Invited)," IEEE J. Lightwave Technol. **23,** 4222-4238 (2005).
5. M. Notomi, A. Shinya, S. Mitsugi, E. Kuramochi, and H. Y. Ryu, "Waveguides, resonators and their coupled elements in photonic crystal slabs," Opt. Express **12,** 1551-1561 (2004).
6. B. E. Little, J. Foresi, G. Steinmeyer, E. R. Thoen, S. T. Chu, H. Haus, E. Ippen, L. C. Kimberling, and W. Greene, "Ultra-compact Si-SiO2 microring resonator optical channel dropping filters," IEEE Photon. Technol. Lett. **10,** 549-551 (1998).
7. V. R. Almeida, C. A. Barrios, R. R. Panepucci, and M. Lipson, "All-optical control of light on a silicon chip," Nature **431,** 1081-1084 (2004).
8. T. Barwicz, M. Popovic, P. Rakich, M. Watts, H. Haus, E. Ippen, and H. Smith, "Microring-resonator-based add-drop filters in SiN: fabrication and analysis," Opt. Express **12,** 1437-1442 (2004).
9. B. E. Little, J. P. Laine, and S. T. Chu, "Surface-roughness-induced contradirectional coupling in ring and disk resonators," Opt. Lett. **22,** 4-6 (1997).
10. S. Noda and T. Baba, *Roadmap on Photonic Crystals*, 1st ed. (Springer, 2003).
11. J. D. Joannopoulos, P. R. Villeneuve, and S. Fan, "Photonic crystals: putting a new twist on light," Nature **386,** 143-149 (1997).

#77652 - $15.00 USD Received 30 November 2006; revised 2 February 2007; accepted 4 February 2007

12. W. Bogaerts, D. Taillaert, B. Luyssaert, P. Dumon, J. Van Campenhout, P. Bienstman, D. Van Thourhout, R. Baets, V. Wiaux, and S. Beckx, "Basic structures for photonic integrated circuits in Silicon-on-insulator," Opt. Express **12,** 1583-1591 (2004).
13. S. G. Johnson, S. Fan, P. R. Villeneuve, J. D. Joannopoulos, and L. A. Kolodziejski, "Guided modes in photonic crystal slabs," Phys. Rev. B **60,** 5751-5758 (1999).
14. Z. Zhang and M. Qiu, "Compact in-plane channel drop filter design using a single cavity with two degenerate modes in 2D photonic crystal slabs," Opt. Express **13,** 2596-2604 (2005).
15. S. McNab, N. Moll, and Y. Vlasov, "Ultra-low loss photonic integrated circuit with membrane-type photonic crystal waveguides," Opt. Express **11,** 2927-2939 (2003).
16. S.-H. Kim, H. Y. Ryu, H. G. Park, G.-H. Kim, Y.-S. Choi, and Y. H. Lee, "Two-dimensional photonic crsytal hexagonal waveguide ring laser," Appl. Phys. Lett. **81,** 2499-2501 (2002).
17. V. Dinesh Kumar, T. Srinivas, A. Selvarajan, "Investigation of ring resonators in photonic crystal circuits", Photonics and Nanostructures **2**, 199-206 (2004).
18. J. Romero-Vivas, D. N. Chigrin, A. V. Lavrinenko, and C. M. Sotomayor Torres, "Resonant add-drop filter based on a photonic quasicrystal," Opt. Express **13,** 826-835 (2005).
19. C. Manolatou, M. J. Khan, S. Fan, P. R. Villeneuve, H. A. Haus, and J. D. Joannopoulos, "Coupling of modes analysis of resonant channel add-drop filters," IEEE J. Quantum Electron. **35,** 1322-1331 (1999).
20. M. Tokushima, H. Yamada, and Y. Arakawa, "1.5-μm-wavelength light guiding in waveguides in square-lattice-of-rod photonic crystal slab," Appl. Phys. Lett. **84,** 4298-4300 (2004).
21. S. Fan, P. R. Villeneuve, J. D. Joannopoulos, and H. A. Haus, "Channel drop tunneling through localized states," Phys. Rev. Lett. **80,** 960-963 (1998).
22. K. Sakoda, "Symmetry, degeneracy, and uncoupled modes in two-dimensional photonic lattices," Phys. Rev. B **52,** 7982-7986 (1995).
23. S. H. Kim and Y. H. Lee, "Symmetry relations of two-dimensional photonic crystal cavity modes," IEEE J. Quantum Electron. **39,** 1081-1085 (2003).

1. Introduction

The optical add-drop filter (ADF) is one of the fundamental building blocks for optical add-drop multiplexers (OADMs), reconfigurable OADMs, optical modulators, and optical switches needed for silicon photonics, photonic integrated circuits (PICs), and wavelength-division multiplexed (WDM) optical communication systems [1-3]. Significant progress has been made on ADF based devices in the areas of compactness, high spectral selectivity, wide spectral tunability, fast switching, and low-power switching [4,5]. One of the most promising designs for waveguided ADFs is the strip-based (or rib-based) micro-ring resonator [2, 6-8], wherein a circulating mode in the ring is excited by the coupling of the forward propagating wave in a nearby bus waveguide. Very high spectral selectivity can be achieved due to the high resonator quality factor Q and the ring's intrinsic single mode nature. Either backward- or forward-dropping of the resonant modes in the ring cavity can be realized by the proper engineering of the bus/ring coupling scheme and by choosing the number of rings within the ADF. To achieve a free-spectral range (FSR) larger than the optical communication window (FSR >30nm for full C-band spectral coverage), a ring radius in silicon of less than 5 μm is required [6]. However, in the strip-based SOI rings, the radiation loss increases exponentially with reduction of the ring radius, which in practice sets a limit on the ring radius of a few micrometers (e.g. 3μm). In addition, the performance of strip-guide micro-ring resonators is highly sensitive to the surface roughness and the nanoscale gap between the ring resonator and the bus waveguide, which creates another challenge in manufacturing [9].

Photonic crystal (PC) structures, on the other hand, can overcome these challenges because, as discussed here, they have the potential to achieve high-Q, low-loss resonators in ultra-compact cavities that are 2x to 4x smaller than the minimum-useable-size strip-based rings. The PC structures offer high spectral selectivity [10-12]. Wavelength-selective active and passive PC devices have been proposed based on various point- and line-defect photonic crystal slab waveguide cavities [10, 13-15]. The first report of a photonic-crystal ring resonator (PCRR) was in a hexagonal waveguide ring laser cavity [16], where flexible mode design and efficient coupling were discussed. Later, the spectral characteristics of the waveguide-coupled rectangular ring resonators in photonic crystals were investigated by

#77652 - $15.00 USD Received 30 November 2006; revised 2 February 2007; accepted 4 February 2007

Kumar *et al*. [17], where a large single quasi-rectangular ring was introduced as the frequency selective dropping elements.

Here we propose and investigate a new type of optical ADF based on ultra-compact PCRRs. We focus on the dielectric rods square lattice PC structure. However, we anticipate that the trends discovered here will apply to other lattice symmetries, such as air hole triangular lattices. In this paper, the ADFs use a combination of line-defect (W1) PC waveguides and single- or dual-PCRRs. We find that high wavelength selectivity is achieved by introducing dielectric scatterers at the corners of square "ring" resonators. Backward-dropping was realized in single-ring PCRRs with dropping efficiency greater than 96%. Surprisingly, both forward- and backward-dropping were demonstrated in double-ring PCRR structures, with forward or backward selected by controlling the coupling of cavity modes with different symmetry and degeneracy. High spectral selectivity with high cavity Q appears feasible, which makes these PCRR based ADFs promising building blocks for electrically controlled modulators and switches.

The basic properties of the PCRRs are introduced in Sec. 2, followed by the design of single-ring PCRR ADFs in Sec. 3. Dual-ring PCRR based ADF design and transmission characteristics will be discussed in Sec. 4, for both forward- and backward-dropping.

2. Photonic crystal ring resonators

Figure 1 shows some examples of PCRRs: a quasi-square ring in a square lattice, a hexagonal ring in a triangular lattice, and a circular ring in a quasi-PC (e.g. the QPC shown with 12-fold symmetry [18]). Compared to point-defect or line-defect PC cavities, PCRRs offer scalability in size and flexibility in mode design due to their multi-mode nature [19]. In strip micro-ring resonators, the whispering gallery modes (WGMs) are supported by the total internal reflection (TIR), which sets the ultimate limit for size reduction. By contrast, the resonant modes in PCRRs are supported by the photonic bandgap, which is more efficient in optical confinement, especially for the wavelength-scale ultra-compact cavities. The smallest PCRR can be a single point-defect cavity, which can be very low loss with extremely high Q and ultrasmall cavity volume [10]. For devices, the choice of the ring size is determined by the desired resonant wavelength, and the tradeoff between the cavity Q and the modal volume V. Shown in Fig. 2 are the modal properties of the quasi-square-rings configured within a square lattice of dielectric rods. The modal volume V is proportional to the ring size, with smaller modal volume V for smaller rings. For PCRR cavities with two different sizes simulated (shown in Fig. 2), high cavity Q factors ($4x10^3$ to $3x10^5$) were obtained. This high Q feature is highly desirable for spectral selectivity and wavelength tunability in the filter and switch design.

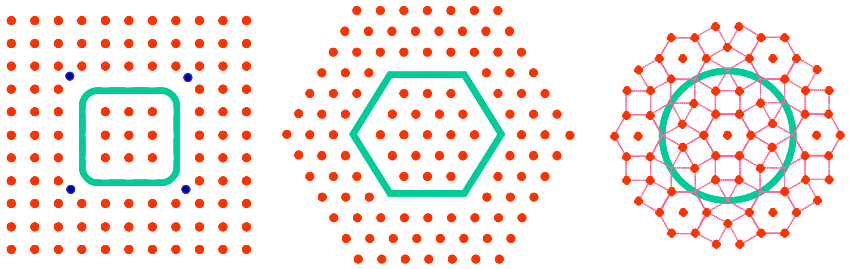

Fig. 1. Photonic crystal ring resonators (PCRRs): (a) Quasi-square ring PCRR in square lattice; (b) Hexagonal ring PCRR in triangular lattice; (c) Circular ring PCRR in quasi-photonic crystal structure (12-fold symmetry as shown).

#77652 - $15.00 USD Received 30 November 2006; revised 2 February 2007; accepted 4 February 2007

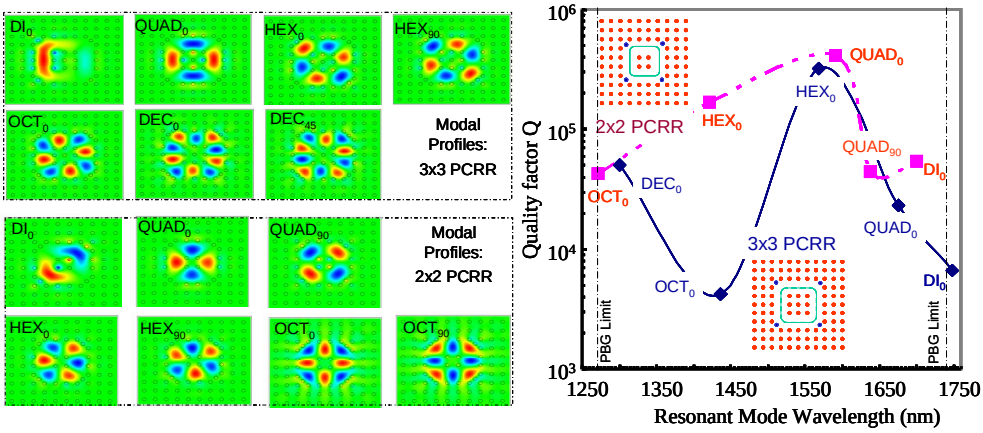

(a) (b)

Fig. 2. Modal properties for the quasi-square PCRRs in a square lattice of dielectric rods: (a) Field pattens of the cavity modes within the spectral range of first photonic bandgap; (b) The corresponding resonant mode wavelengths and the quality factor Qs for these modes in both 3x3 and 2x2 PCRRs. The different modes are: dipole (DI), quadrupole (QUAD); hexapole (HEX), octupole (OCT), and decapole (DEC). The modal degeneracy is denoted with the subscript "0" and "90" (or "45").

3. Single ring photonic crystal ring resonators

All the designs in this paper are based on two-dimensional (2D) square lattice dielectric-column photonic-crystal structures [3, 20], as shown in Fig. 1(a), where the refractive index of dielectric rods, n_h, is 3.59, surrounded by the background of air (n_l=1.00). This choice is meant to simulate the behavior of a silicon-on-insulator PC structure operating at telecomm wavelengths. Although the real SOI structure, would, in practice, require 3D analysis, our 2D approach gives a general indication of the expected 3D behavior. 2D analysis carried out here allows us to identify qualitatively many of the issues in the cavity design (e.g. mode control, cavity Q and the placement of the scatterers in our quasi-square ring cavity) and the coupling scheme design (e.g. the placement of the ring and the W1 defect waveguide, the relative coupling and symmetric impact). This can offer us the design trade-offs and guidelines before the real structure design based on a completely 3D FDTD technique, which is typically computational time and memory consuming.

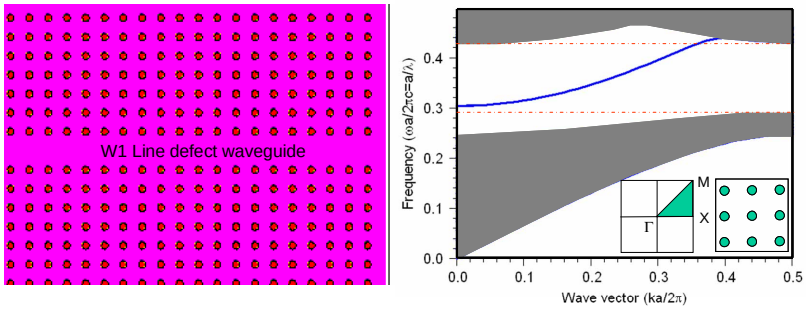

(a) (b)

Fig. 3. (a) Single line-defect (W1) photonic crystal waveguide; (b) Dispersion plot and the corresponding defect mode shown as a blue line) in the photonic bandgap region.

In this investigation, the ratio of the rod radius r to the lattice constant a, is 0.185. The photonic bandgap and the dispersion curve for the guided defect mode in the single line-defect

#77652 - $15.00 USD Received 30 November 2006; revised 2 February 2007; accepted 4 February 2007

waveguide (W1, missing one row of rods along the ΓX direction) are shown in Fig. 3. There exists a single-mode frequency (normalized) ranging from 0.303 to 0.425. For the 1550 nm communication window, the lattice constant, *a*, is set as 540 nm. Thus the W1 PC waveguide is broadband, with guided single-mode spans from 1270 to 1740 nm (between the two vertical dash lines in Fig. 2(b)). On the other hand, the ultra-compact PCRR cavity supports one or only a few cavity modes, mostly WGM modes, with their specific spectral locations controlled by the cavity design (the structural parameters). The resonance wavelengths are tunable by means of a localized change in the dielectric lattice's refractive index. It is worth noting that in principle all the modes supported by the PCRR cavity, whether they are WGM modes or not, can all be applied to the filter design.

In all the designs, we have introduced four dielectric-rod scatterers, one in each corner of the quasi-square ring. These rods are labeled as "s" with blue color, and each is located in the center of its four nearest-neighbor rods. These scatterers have exactly the same diameters and refractive indexes as all other dielectric rods in the PC structure. These scatterers were introduced by Kumar *et al.* as well, in order to suppress the counter propagating modes which can cause spurious dips in the transmission spectrum [17]. We put in these s-rods to improve the spectral selectivity and give a near-ideal drop efficiency.

The single ring optical ADF is schematically shown in Fig. 4(a), where the incident port and exit ports are labeled as A, B, C, D, respectively. The transmission characteristics were simulated with the two-dimensional finite-difference time-domain (FDTD) technique using perfectly matched layers (PML) as absorbing boundaries. A Gaussian optical pulse, covering the whole frequency-range-of-interest, is launched at the input port A. Power monitors were placed at each of the other three ports (B, C, D) to collect the transmitted spectral power density after Fourier-transformation. All of the transmitted spectral power densities were normalized to the incident light spectral power density from input Port A.

Shown in Fig. 4(b) are the normalized transmission spectra for three output ports (B, C, D) in the single ring ADFs. Note that, for a cavity *without* scatterers (four dielectric rods labeled as "s" in Fig. 4(a)), a low drop efficiency with poor spectral selectivity was obtained. By simply introducing four scatterers, significantly improved spectral selectivity, with close to 100% (>98%) drop efficiency, can be achieved at the resonant frequency (1567nm in this case). Snapshots of the electric field distribution in the ADF for through (off-resonance: λ_0=1500 nm) and drop (on-resonance: λ_1=1.567 μm) channels are shown Fig. 4(c).

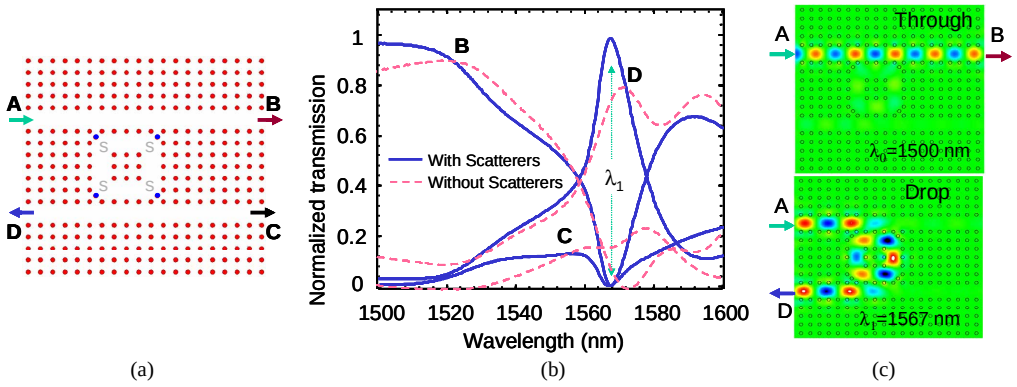

Fig. 4. (a) Single-ring PCRR ADF; (b) normalized transmission spectra at three output ports B, C, D for PCRRs with and without scatterers; (c) The electric field patterns for the through (off-resonance: λ_0=1500 nm) and drop (on-resonance: λ_1=1567 nm) channels.

It is worth mentioning that the Q of this single-ring ADF is only ~160 (Q=λ/δλ). A desirable filter operating in the wavelength range of 1300nm to 1550nm would require a much higher Q, on the order of 1500 or higher, to achieve a linewidth of 1nm or less for the

#77652 - $15.00 USD Received 30 November 2006; revised 2 February 2007; accepted 4 February 2007

wavelength range of 1300 to 1550nm. Such Q values can be achieved routinely in air hole two-dimensional photonic crystal slab-based defect mode cavities for various lasing and switching applications. Theoretically the Q value for the ideal single-ring (3x3) PCRR can be greater than 10^5 (as shown in Fig. 2(b)). Q values greater than 2000 were obtained experimentally in an air-hole-based hexagonal ring cavity laser as well [16]. The discrepancy between the ideal PCRR Q and the ADF Q is mainly due to the weak confinement in the coupling sections between the W1 waveguide and PCRR ring. As shown in Fig. 5, higher spectral selectivity can be achieved with Q greater than 1000 in the modified single-ring PCRR-based ADF by simply increasing the coupling section periods between the W1 waveguide and the PCRR (from one period in Fig. 4 to two in Fig. 5). However, the dropping efficiency decreased to 80%. In general there is a trade-off between the increase of the cavity Q and the decrease of the coupling/dropping efficiency. Based on the Q factors shown in Fig. 2b, to maintain high drop efficiency (>98%), higher Q factors (>2000) can be obtained in these ADF designs, with further optimization processes such as the coupling section engineering (e.g. bended waveguide for different coupling length), PCRR cavity Q tuning (e.g. dielectric rod size and location adjustment), and/or different PCRR configurations (dielectric rod or air hole PC structures for different ring cavities shown in Fig. 1).

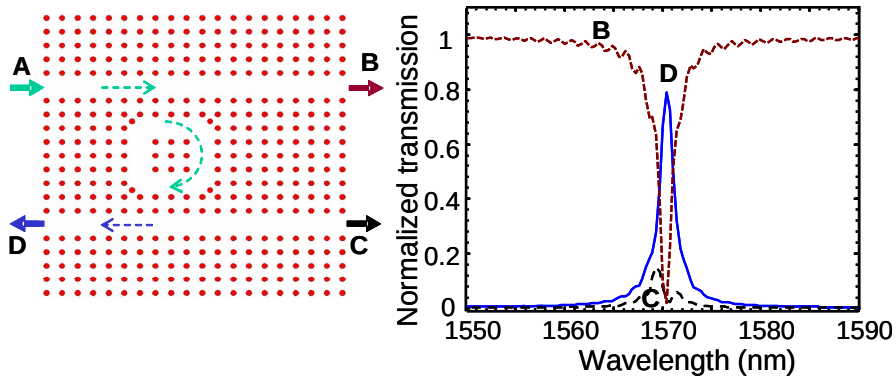

Fig. 5. Single-ring PCRR based ADF with higher spectral selectivity (Q>1000, $\delta\lambda$=1.5nm at λ_1=1571nm), by increasing the coupling periods between W1 waveguide and PCRR cavity from one to two.

4. Dual-ring photonic crystal ring resonators

By coupling resonators, one can modify the transfer characteristics achievable with a single-ring resonator. Forward dropping can be achieved in dual ring configurations, as demonstrated in the micro-ring based OADMs. Here, based on the basic building blocks of single-ring PCRRs, dual-ring PCRR-based OADMs were analyzed for forward dropping *as well as* backward dropping, with the control of mode symmetry and ring coupling.

For the weakly coupled dual ring PCRRs, as shown in Fig. 6(a), where the coupling periods (defined as the number of the shared dielectric rods) were 2*a* (*a* is the lattice constant), backward dropping was achieved. Comparing that dropping with the backward dropping characteristics obtained from single-ring PCRRs shown in Fig. 4, higher spectral selectivity was obtained with the Q approaching 200 for the dropping channel.

For the strong coupling case, as shown in Fig. 7, where the coupling period increased to 4a, forward dropping was obtained, similar to the case of strip-based dual micro-ring resonator ADFs. However, here the dropping channels switched to the other two resonant-cavity modes with different symmetry properties (at 1558nm and 1574nm). This is caused by the mode superposition. At resonance, the resonant field couples to the drop and the input guides. The ring cavity power that couples back into the input guide does so in antiphase with the input signal, resulting in cancellation at the throughput port and making complete power transfer from the input to the drop port possible.

#77652 - $15.00 USD Received 30 November 2006; revised 2 February 2007; accepted 4 February 2007

This flexible design of backward and forward dropping is one of the advances in photonic crystal based resonators, which follows from PC electromagnetic mechanisms that differ from those employed in micro-ring resonators. In micro-ring resonators, the behavior is typically based on phase-matched coupling between orbiting waves in the ring and propagating modes in the waveguide. The wave propagation inside that ring is governed by the total internal reflection (TIR) principle, and the micro-ring resonator is side-wise evanescently coupled to the waveguide. The propagation direction inside the ring resonator is determined by mode coupling in space and is always taken to be the same direction as that of the incident wave [20]. This is true for the coupling between waveguide and the ring resonator, and also for the coupling between ring resonators. Backward dropping and forward dropping can be realized with an odd number and an even number of coupled ring resonators, respectively.

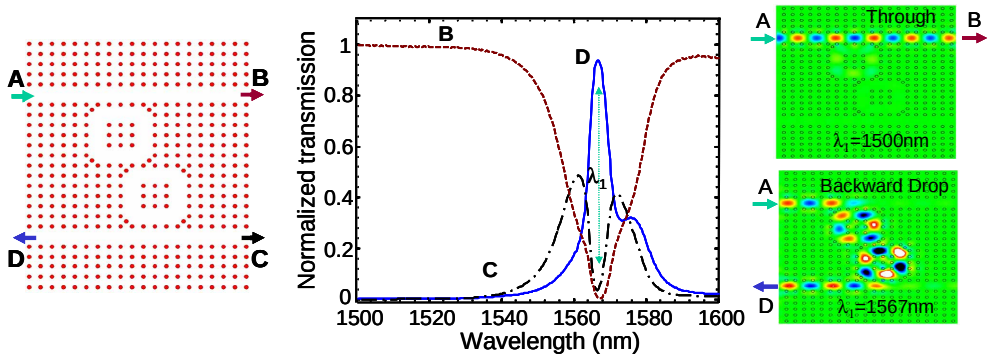

Fig. 6. Dual-ring PCRR ADF for backward-dropping: (a) Schematic showing the weakly coupled dual PCRR rings with coupling period of 2a; (b) Normalized transmission spectra; (c) The field patterns of electric field distribution for "through" (off-resonance: λ_0=1500nm) and "backward drop" (on-resonance: λ_1=1567nm)channels.

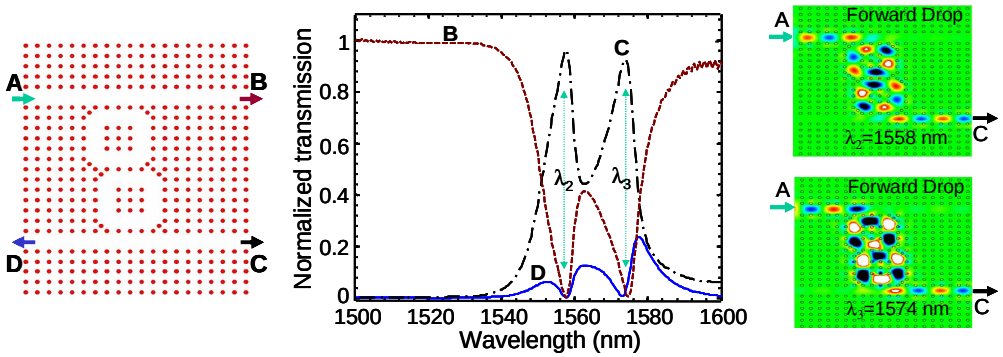

Fig. 7. Dual-ring PCRR ADF for forward-dropping: (a) Schematic showing the strongly coupled dual PCRR rings with coupling period of 4a; (b) Normalized transmission spectra; (c) The field patterns of electric field distribution for two "forward drop" channels (on-resonance: λ_2=1558 nm, λ_3=1574 nm).

However, the determining principle for wavelength-size photonic crystal cavities in general can no longer be characterized as the propagating states, and the idea of phase-matching coupling may not be applicable here. Instead, photonic-crystal resonant- cavity coupling can be analyzed based on the resonant state symmetry and degeneracy in both the real and imaginary parts of the frequency, proposed by Fan *et al* [21]. The PCRR resonant coupling occurs due to the frequency and phase matching between the propagating waveguide mode and the PCRR resonant cavity mode. The coupling direction is mainly determined by the modal symmetry and the relative coupling between the PCRRs. The direction is the same

#77652 - $15.00 USD Received 30 November 2006; revised 2 February 2007; accepted 4 February 2007

for the propagating wave in the waveguide and the coupled wave inside PCRR. However, the direction may be the same or reverse for the coupling between PCRRs, depending upon the coupling strength and the modal symmetry [22, 23]. Both forward dropping and backward dropping can be obtained depending upon the mode-symmetry properties with respect to the coupling configurations.

We attempted to understand this with the movies in Fig. 8 that show the propagation direction of different modes in dual-ring PCRRs. In Fig. 8(a), the maximum coupling efficiency occurs at λ_1=1567nm, along the ΓM direction, with the field minimum and maximum alternatively coupled. Modes propagate clockwise in both PCRR rings, which results in backward-dropping. On the other hand, a pair of doubly degenerate modes at λ_2=1558nm and λ_3=1574nm appeared to have maximum coupling efficiency in the strongly coupled dual-ring cavities, along the ΓX direction, where both "even-mode-like" ("+" to "+" in Fig. 8(b)) and "odd-mode-like" ("+" to "-" in Fig. 8(c)) .. The coupled mode in the second PCRR ring cavity propagates counter-clockwise, which leads to the forward-dropping. If the above analysis is true, this opens up additional design flexibility with the desired or optimal coupling attained simply by simply shifting the multi-PCRRs along different directions.

The dual-ring ADFs shown in Fig. 6 and Fig.7 are excellent structures with which to realize 1 x 1 modulation, 1 x 2 switching, 2 x 2 switching and reconfigurable WDM [1]. The modulation, switching and reconfiguration would be obtained by perturbing the refractive index of rods in dielectric rods lattice structures, or the refractive index of the semiconductor slabs in the air-hole lattice structures. Shown in Fig. 9 is the PCRR resonant cavity peak wavelength shift with the change of the refractive index, for both air hole and dielectric rod based PC structures. For a refractive index change of 0.002 (e.g. based on fast free carrier plasma dispersion effect on Si [1], wavelength shift of 1nm is feasible in air hole PCRR based structures. An electrooptical switch can be realized with high suppression ratio with the cavity Q factor greater than 2000 and a center wavelength around 1550nm.

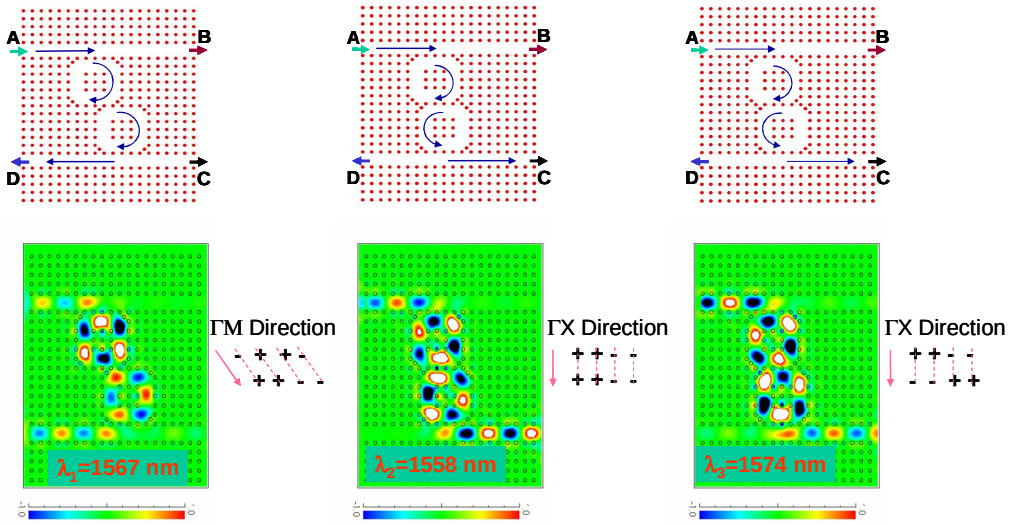

Fig. 8. Comparison of Backward- and forward-dropping with the movies shown the different modal propagation directions due to the coupling difference and the modal symmetry. The coupling field relations are labeled with "+" and "-" signs for either even or odd modal coupling. (Movies 612KB, 625KB, 666KB).

#77652 - $15.00 USD Received 30 November 2006; revised 2 February 2007; accepted 4 February 2007

5. Summary

In summary, we proposed a new class of ultra-compact optical add-drop filters based on photonic- crystal ring resonators. More than 96% drop efficiency can be obtained with the modal quality factor Q varying from 160 to over 10^3. Both backward- and forward-dropping can be achieved in dual-ring PCRRs as selected by different coupling schemes for the optical coupling of different resonator modes based on the modal symmetry. Such structures offer new and promising building blocks for ultra-compact scalable photonic integrated circuits based on photonic crystals and other nanophotonic structures.

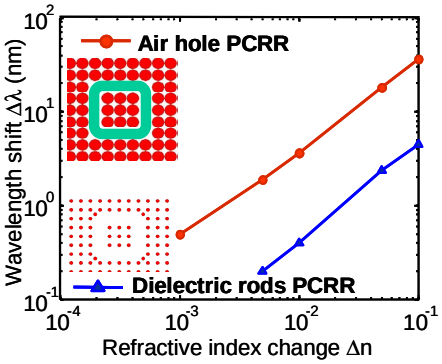

Fig. 9. The resonant cavity peak wavelength shifts with the change of the refractive index Δn. The perturbation sections are the ring section (green colored) for air hole PCRRs and the inner dielectric rods (3x3) for dielectric rod PCRR structures.

Acknowledgments

This work was supported in part by the U.S. Air Force Office of Scientific Research under Grant FA9550-06-1-0482, and in part by National Science Foundation under Grant DMI-0625728.

#77652 - $15.00 USD Received 30 November 2006; revised 2 February 2007; accepted 4 February 2007